Scientific Contributions Oil & Gas, Vol. 47. No. 3, December: 341 - 360

SCIENTIFIC CONTRIBUTIONS OIL AND GAS

Testing Center for Oil and Gas

LEMIGAS

Journal Homepage:http://www.journal.lemigas.esdm.go.id

ISSN: 2089-3361, e-ISSN: 2541-0520

The Effect of CO_2-Brine-Rock Interaction Towards Sand Onset Modeling in Dolomite-Rich Sandstone: A Case Study in Air Benakat Formation, South Sumatera, Indonesia

Prasandi Abdul Aziz[1,3], Bagus Endar Bachtiar Nurhandoko[2,4], Taufan Marhaendrajana[1,3], Utjok W.R. Siagian[1,3] and Tutuka Ariadji[1,3]

[1]Department of Petroleum Engineering, Faculty of Mining and Petroleum Engineering, Institut Teknologi Bandung
Ganesha Street No. 10, Bandung 40132, Indonesia, Indonesia.

[2]Department of Physics, Faculty of Mathematics and Natural Sciences, Institut Teknologi Bandung
Ganesha Street No. 10, Bandung 40132, Indonesia, Indonesia.

[3]Research Center for CO2 and Flare Gas Utilization, Institut Teknologi Bandung
Ganesha Street No. 10, Bandung 40132, Indonesia, Indonesia.

Corresponding author: andreteu191102@gmail.com.

Manuscript received: July 15th, 2024; Revised: September 20th, 2024
Approved: November 11th, 2024; Available online: December 18th, 2024.

ABSTRACT - Carbon Capture Utilization Storage (CCUS) into geological storage (e.g., Enhanced Oil or Gas Recovery) provides a solution to reduce CO¬2 emissions. However, it still remains a potential operational problem, such as sand problem phenomena in producer wells. This study observes the phenomenon of sand problems in production wells possibly triggered by CO_2-brine-rock interactions on CO_2 injection in rich dolomite sandstone reservoir. This research performs several experimental works (i.e., time-lapse dry mass measurements, X-Ray Diffraction (XRD), Scanning Electron Microscope (SEM), and elastic wave measurements) by using CO_2-brine-rock batch experimental setup as well as geochemical simulation to observe mineral dissolution, pore structures alteration as well as rock physics alteration due to CO_2-brine-rock interactions. We used an outcrop sample of dolomite-rich sandstone from the Air Benakat Formation, South Sumatera, Indonesia. Our experimental and simulation works show that dolomite dissolution (dolomite reduction of ~4% after 14 soaking days), secondary porosity development (11% of visible porosity improvement), as well as rock strength reduction, occur indirectly (shown by elastic wave velocity, i.e. V_p and V_s reduction of ~3.8% and ~4.4%, respectively) due to CO_2-brine-rock interactions. Subsequently, the results of elastic wave velocity measurements were then used to modify a considerable sand onset prediction (sand-free envelope) model. The modified model showed that the production well was more prone to sand problems due to CO_2-brine-rock interactions. Thus, it is concluded that the sand onset prediction model with considering CO_2-brine-rock interactions could help to design a better sand management strategy in producer wells.

Keywords: CO_2-brine-rock interactions, CCUS, dolomite-rich sandstone, sand problem

How to cite this article:

Prasandi Abdul Aziz, Bagus Endar Bachtiar Nurhandoko, Taufan Marhaendrajana, Utjok W.R. Siagian and Tutuka Ariadji, 2024, The Effect of CO2-Brine-Rock Interaction Towards Sand Onset Modeling in Dolomite-Rich Sandstone: A Case Study in Air Benakat Formation, South Sumatera, Indonesia, Scientific Contributions Oil and Gas, 47 (3) pp. 341-360. DOI. org/10.29017/SCOG.47.3.1649.

INTRODUCTION

One of the solutions to reduce CO_2 emissions into the atmosphere is by injecting CO_2 into geological storage for sequestering CO_2 (IPCC, 2005). In Indonesia, the feasibility of CCUS projects have been studied by several reseachers (Sugihardjo, 2022; Aziz, et al., 2023)et al., 2023 alongside CO2 hub-clustering management (Nugraha et al., 2024). The illustration of CO_2 injection in the aquifer that could potentially lead to an acidic environment near the producer well is depicted in Figure 1. This acidic environment may lead to production problems, such as sand problems.

The effects of pressure and temperature on CO_2 solubility in water have been observed by previously reported experimental studies (Enick & Klara, 1990; Spycher et al., 2003). When CO_2 is soluble in water, it creates carbonic acid which is mild acid with pH ranging from 4-5 (Greenwood & Earnshaw, 1997; Lerman & Mackenzie, 2018; Mitchell et al., 2010)2018; Mitchell et al., 2010.

$$CO_2 + H_2O \leftrightarrow H_2CO_3 \quad (1)$$

Carbonic acid can also react with certain reservoir rock minerals and cause dissolution, such as calcite (Buhmann & Dreybrodt, 1985; Dreybrodt & Kaufmann, 2007)

$$CaCO_3 + H_2O + CO_{2(aq)} \leftrightarrow Ca^{2+} + 2HCO_3^- , \quad (2)$$

$$CaMg(CO_3)_2 + 2H^+ \leftrightarrow Ca^{2+} + Mg^{2+} + 2HCO_3^- \quad (3)$$

$$SiO_2 + 4H^+ \leftrightarrow Si^{4+} + 2H_2O . \quad (4)$$

The dissolution rate of minerals (including calcium and magnesium) is influenced by the pH of the solution (Casey & Sposito, 1992; Matter et al., 2007; Black et al., 2015)2015, temperature (Casey & Sposito, 1992), CO2 partial pressure and rock surface area (Luquot et al., 2014; Black et al., 2015; Lamy-Chappuis et al., 2016).

Extensive experiments on rock strength alteration due to CO2-brine-rock interaction have been done under several studies (e.g. Al-Ameri et al., 2016; Rathnaweera et al., 2017; Yu et al., 2019)the effect of the storage time on these properties is investigated. In this study, CO2 was injected into the brine-soaked core samples under simulated downhole conditions of high pressure and high temperature (2000 psi and 100 °C. However, to the best of the author's knowledge, research on sand problems due to CO2-brine-rock interactions is still limited.

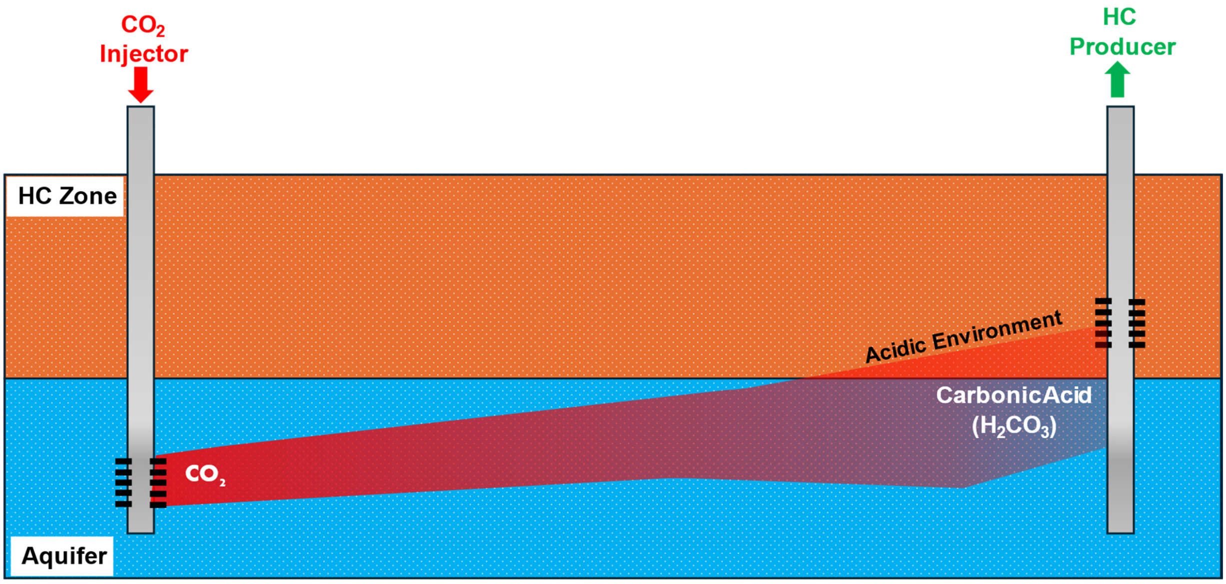

Figure 1
Illustration of CO_2 injection in aquifer that could potentially lead to acidic environment near producer well due to carbonic acid

In this study, practical sand onset criteria proposed by (Willson et al. 2002; Vaziri et al. 2002 and Palmer et al. 2003) would be used to observe the impact of CO_2-brine-rock interaction on the sand onset problem. The model was based on a rock stress model with shear failure criteria, assuming that rocks are linear elastic. Sand production was assumed to occur at the time when the maximum value of the effective tangential stress around the perforation exceeds the effective strength of the formation rock (in some literature, the strength of the formation rock can be analogized as the Unconfined Compressive Strength (UCS), Thick-Walled Cylinder (TWC), or the empirical function of TWC) (B. E. B. Nurhandoko & Listyobudi 2018; B. E. B. Nurhandoko et al. 2021). This study emphasizes rock physics alteration due to CO_2-brine-rock interaction that hypothetically may affect rock strength. Several experimental studies have been demonstrated to investigate mineral dissolution mechanisms and elastic wave velocity alteration after a rock sample was soaked by CO_2-brine. Elastic wave velocity indirectly correlates with rock strength (such as Young's modulus) which dominantly affects sand problems in producer wells. Thus, (Wilson et al. 2002) model would be used to observe the impact of CO_2-brine-rock interaction on the sand prediction model, especially in dolomite-rich sandstone.

METHODOLOGY

Experimental Material and Methods

This study experimental setup & methodology is explained in Figure 2. Air Benakat Formation (ABF) sandstone outcrop sample in the South Sumatera basin was used in this study. ABF sandstone porosity and permeability typically range between 16-18% and 10-3000 mD, respectively (Barber et al. 2005; Bishop 2001). The samples were similar to the previously reported study (Aziz et al. 2023). Based on X-ray diffraction (XRD) measurements (using Rigaku SmartLab X-ray Diffraction after the samples were prepared in powder form with 200 mesh size), ABF samples used in this study consist of dolomite (79%), quartz (17%), and kaolinite (4%). Based on a nearby analog well (P-3) at ABF interval, it is known that water salinity is 15000 mg/L, pore pressure is 1300 psi and vertical stress is 2500 psi.

To achieve the objectives of this study, two types of rock sample forms are required, i.e., small cube and cylindrical samples. Small cube samples were used for observing chemical or dissolution effects, such as dry mass (using Fujitsu FSR-A Precision digital mass balance with a capacity of 220 g and precision of 0.001 g), XRD and Scanning Electron Microscope (SEM using JEOL JSM 6510 LA) measurements, while cylindrical sample was used for observing rock mechanics alteration, i.e. elastic wave velocity (P & S wave or V_p^ and V_s^ using pressurized SeisCore (Nurhandoko 2022) tool. All measurements were conducted at room temperature (270C ± 30C).

All samples were soaked in a CO2-brine-rock batch apparatus as shown in Figure 2. This apparatus consists of a mixing reactor (to mix CO2 and brine), a soaking reactor (to soak rock samples), a fluid tap (to measure pH solution), a pump, a pressure gauge, and valves. Subsequently, the rock samples were then immediately put into a sealed plastic container (to prevent contamination). Artificial brine was used by mixing 15 g of NaCl (chemical pure grade, purity ≥ 99%, form: white crystalline solids) and 1.0 L of demineralized water with a magnetic stirrer for about 15-30 minutes with 60 rpm to obtain homogeneous NaCl solution.

To observe CO_2-brine-rock interactions toward rock mechanics, a non-destructive test, namely elastic wave velocity (P & S wave) was conducted. Prior to the measurements, the sample was saturated with artificial brine for 1 day and then "dried" until it reached irreducible water saturation by using centrifuge (using Damon IEC Division HN-S Centrifuge with a maximum speed of 4150 rpm) following reported procedures and standards (API RP40 1998; Slobod et al. 1951; McPhee et al. 2015). This procedure was conducted to avoid biased measurements of whether elastic wave velocity alteration was caused by fluid saturation (Gutierrez et al. 2020; Nakajima & Xue 2021) or rock properties alteration.

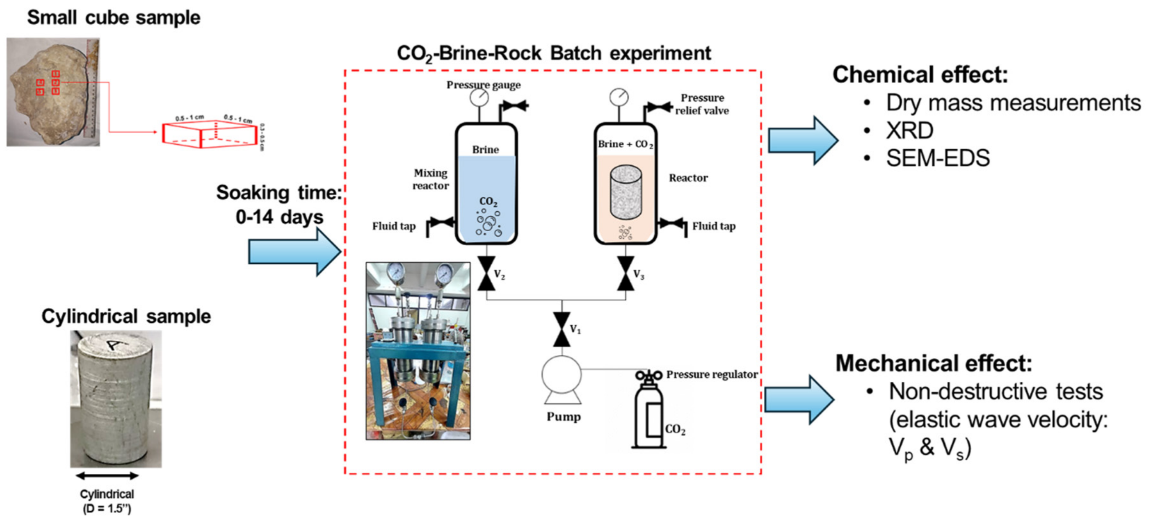

Figure 2
Experimental setup and methodology

Geochemical Simulation

A geochemical simulation, namely TOUGHREACT, was used to simulate CO2-brine-rock interactions that can simulate non-isothermal multiphase reactive geochemical transport (Xu et al., 2006; Zhang et al., 2006; Xu et al., 2014). XRD results were used to determine initial rock mineral compositions. Porosity (ϕ) alteration is based on (Xu et al., 2006).

$$\phi = 1 - \sum_{m=1}^{m} fr_m - fr_u \tag{5}$$

where m is the numbers of minerals, fr_m is m mineral volume fraction in rock, and fr_m is the non-reactive rock volume fraction. Kinetic parameters rate constant (k_25), activation energy (E_a), and power term (n) for each mechanism are listed in Table 1 (Xu et al., 2006).

Table 1
Reactive surface area and parameters for kinetic rate law for specific minerals (Xu et al., 2006)

Mineral	Reactive Surface Area A (cm²/g)	Parameters for kinetic rate law: Neutral Mechanism		Acid Mechanism			Base Mechanism		
		k_{25} (mol/m²/s)	E_a (KJ/mol)	k_{25}	E_a	n (H^+)	k_{25}	E_a	n (H^+)
Quartz	9.8	1.023×10^{-14}	87.7						
Kaolinite	151.6	6.918×10^{-14}	22.2	4.898×10^{-12}	65.9	0.777	8.913×10^{-18}	17.9	-0.472
Calcite							*Assumed at equilibrium*		
Illite	151.6	1.660×10^{-13}	35	1.047×10^{-11}	23.6	0.34	3.020×10^{-17}	58.9	-0.4
Oligoclase	9.8	1.445×10^{-12}	69.8	2.138×10^{-10}	65	0.457			
K-feldspar	9.8	3.890×10^{-13}	38	8.710×10^{-11}	51.7	0.5	6.310×10^{-12}	94.1	-0.823
Na-smectite	151.6	1.660×10^{-13}	35	1.047×10^{-11}	23.6	0.34	3.020×10^{-17}	58.9	-0.4
Chlorite	9.8	3.02×10^{-13}	88	7.762×10^{-12}	88	0.5			
Hematite	12.9	2.512×10^{-15}	66.2	4.074×10^{-10}	66.2	1			
Magnesite	9.8	4.571×10^{-10}	23.5	4.169×10^{-7}	14.4	1			

Table 1 (continued)
Reactive surface area and parameters for kinetic rate law for specific minerals (Xu et al., 2006)

Mineral	Reactive Surface Area A (cm^2/g)	Parameters for kinetic rate law: Neutral Mechanism		Acid Mechanism			Base Mechanism		
		k_{25} (mol/m²/s)	E_a (KJ/mol)	k_{25}	E_a	n (H^+)	k_{25}	E_a	n (H^+)
Dolomite	9.8	2.951×10^{-8}	52.2	6.457×10^{-4}	36.1	0.5			
Low-albite	9.8	2.754×10^{-13}	69.8	6.918×10^{-11}	65	0.457	2.512×10^{-16}	71	-0.572
Siderite	9.8	1.260×10^{-9}	62.76	6.457×10^{-4}	36.1	0.5			
Ankerite	9.8	1.260×10^{-9}	62.76	6.457×10^{-4}	36.1	0.5			
Dawsonite	9.8	1.260×10^{-9}	62.76	6.457×10^{-4}	36.1	0.5			
Ca-smectite	151.6	1.660×10^{-13}	35	1.047×10^{-11}	23.6	0.34	3.020×10^{-17}	58.9	-0.4
Pyrite	12.9	2.818×10^{-5}	56.9	3.02×10^{-8}	56.9	-0.5			

Sand Onset Modelling

The sand onset criteria were given by (Willson et al. 2002) as follows:

$$P_{wf} \geq CBHFP = \frac{3S_1 - S_3 - S_y}{(2-A)} - P_r\frac{A}{(2-A)} \quad (6)$$

where is well flowing bottom hole pressure (psi), and are major and minor principal stress (psi), is effective rock strength (psi), is average reservoir pressure (psi) and is poroelastic constant as a function of Poisson's ratio () and Biot's constant () as follows:

$$A = \frac{(1-2v)\alpha}{(1-v)} \quad (7)$$

α is usually assumed to be equal to 1 (Zoback 2007). Dynamic Poisson's ratio () can be derived from compressional wave or P wave velocity () and shear wave or S wave velocity () as follows (Zoback 2007):

$$v = \frac{V_p^2 - 2V_s^2}{2(V_p^2 - V_s^2)} \quad (8)$$

Young's modulus can be derived as follows (Zoback 2007):

$$E = \frac{\rho(V_p^2 - 2V_s^2)(1+v)(1-v)}{v} \quad (9)$$

where is bulk density (gr/cm3).

The illustration of sand onset criteria by applying Eq. 6 is depicted in Figure 3.

The workflow of sand onset model construction by utilizing elastic wave velocity measurements is shown in Figure 4. Dynamic Poisson's ratio (v) is calculated by using Eq. 8. Previous studies have constructed empirical equations for estimating minimum stress S_{hmin} (Hubbert & Willis 1957; Matthews & Kelly 1967; Eaton 1969; Breckels & Van Eekelen 1982; Zoback & Healy 1984; Holbrook et al. 1995; Holbrook et al. 1995). This study used the Eaton correlation to estimate S_{hmin} as a function of Poisson's ratio (v) as follows (Eaton, 1969):

$$S_{hmin} = \left(\frac{v}{1-v}\right)\left(S_v - P_p\right) + P_p \quad (10)$$

From the analog P-3 well, it is determined that the faults regime in ABF at the observed interval is strike-slip (). Jaeger & Cook (1979) have developed a relation between effective stress, pore pressure, and friction coefficient as follows

$$\frac{\sigma_1}{\sigma_3} = \frac{S_{Hmax} - P_p}{S_{hmin} - P_p} = \left[(\mu^2+1)^{\frac{1}{2}} + \mu\right]^2 \quad (11)$$

where is the friction coefficient. Byerlee (1978) has conducted laboratory experiments about for different spectrums of rock types and has come to the conclusion that ranges between 0.6 – 1.0 (0.6 ≤ ≤ 1.0). Jaeger & Cook (1979) stated that the typical value of rock friction coefficient is 0.6. For simplification, we used in Eq. 11, and obtained (Jaeger & Cook, 1979):

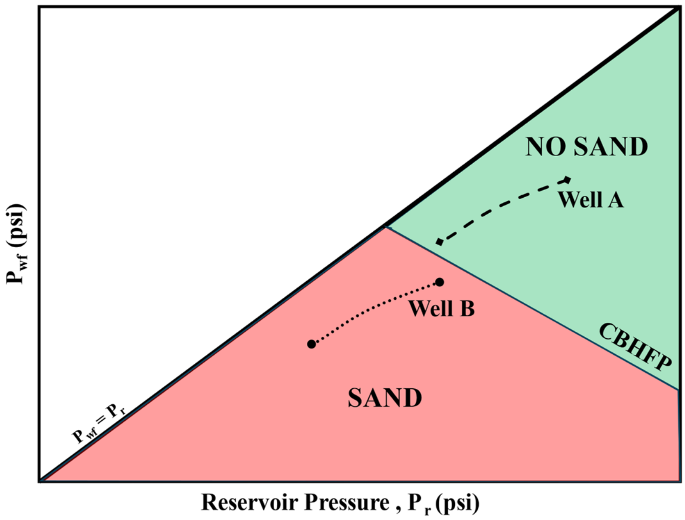

Figure 3
Illustration of CBHFP sand onset criteria (Eq. 6). Well A pressure profile shows that most likely it will be safe from sand problem (green area or above CBHFP). On the other hand, well B shows that most likely sand problem will be occurred (red area or below CBHFP)

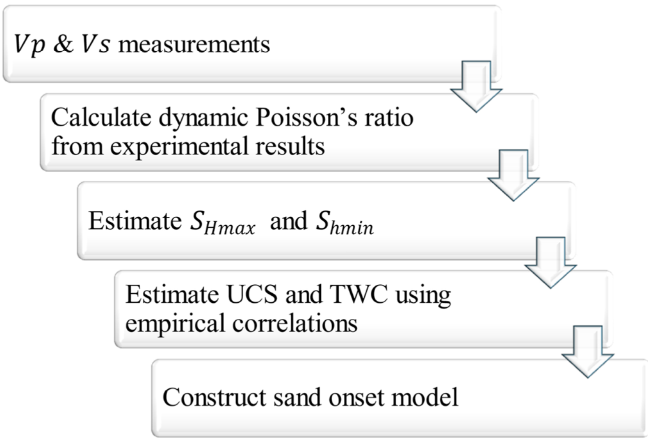

Figure 4
Workflow to construct sand onset model

$$S_{Hmax} = 3.119\left(S_3 - P_p\right) + P_p. \quad (12)$$

Since we have limited core samples, empirical correlations were used to estimate rock strength properties, i.e. UCS and TWC, from elastic wave velocity measurements. An extensive literature review of 31 empirical correlations between UCS and physical rock properties has been conducted and summarized by (Chang et al. 2006), for elastic velocity, Young's modulus and porosity for sandstone (Bradford et al. 1998; Moos et al. 1999; Fjaer 2008), limestone & dolomite (Golubev & Rabinovich 1976; Militzer & Stoll 1973) and shale (Lal 1999; Horsrud 2001). From XRD results, it is determined that ABF is dominated by dolomite, so (Golubev & Rabinovich 1976) correlation for dolomite or limestone was selected to estimate UCS as follows:

$$UCS = 10^{2.44 + \frac{109.14}{\Delta t}} \quad (13)$$

where UCS is unconfined compressive strength (in MPa) and Δt is $\frac{1}{V_p}$ (in).

More than 20 empirical correlations of TWC as functions of UCS and porosity have been compared by Khaksar et al. (2018). Thus, Rahman et al. (2010) correlation was selected which represented tertiary weak/intermediate rocks in Southeast Asia as follows:

$$TWC = 114.9\ UCS^{0.52}. \quad (13)$$

Then, this TWC value was later used as in Eq. 6 to construct the sand onset model.

RESULTS AND DISCUSSION

Experimental Results

Dry mass measurements

Dry mass measurements showed that sample mass reduction (~1.4%) was observed after it was soaked by CO_2-brine for 14 days, as depicted in Figure 5. From this observation, mineral dissolution most likely appears to have occurred due to CO_2-brine-rock interactions.

XRD

From XRD measurements, it is evident that samples dominantly consisted of dolomite (highest peak intensity) with quartz and a small amount of kaolinite, as depicted in Figure 6. It was also observed that significant peak intensity differences between samples without CO2 treatment (red line) and after soaking by CO2-brine for 14 days (black line) were not significant. It also explained that CO2-brine-rock interactions did not reactively form new mineral precipitations. XRD quantitative analysis indicates dolomite dissolution (~4% dolomite wt.% reduction), as shown in Table 2.

Table 2
XRD quantitative analysis

Mineral	No CO_2 treatment	CO_2 soaking time (14 days)
Dolomite	79%	75%
Quartz	17%	21%
Kaolinite	4%	4%

SEM

SEM measurements for ABF rock samples are depicted in Figure 7. The intercrystalline porosity of the dolomite crystal (green square) is shown in Figure 7(a). Meanwhile, secondary porosity development after it was soaked by CO2-brine for 14 days is shown in Figure 7(b). Visible or surface porosity was calculated by using image processing software (ImageJ) whereas dark area was calculated as porous, as shown in Figure 8 and Figure 9. It shows that visible porosity was significantly improved (~11%) which indicates mineral dissolution after being soaked by CO2-brine. However, these results may have uncertainties regarding the heterogeneity of rock samples even though samples were taken from nearby locations.

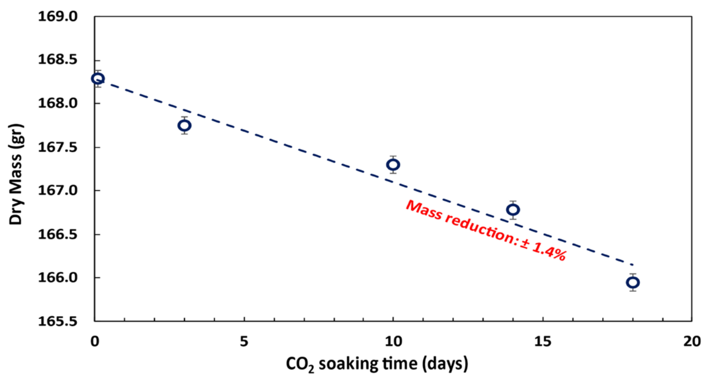

Figure 5
Dry mass measurement

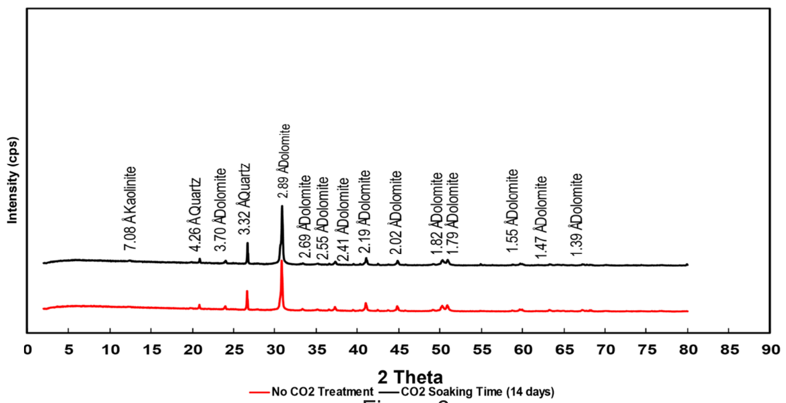

Figure 6
XRD measurement

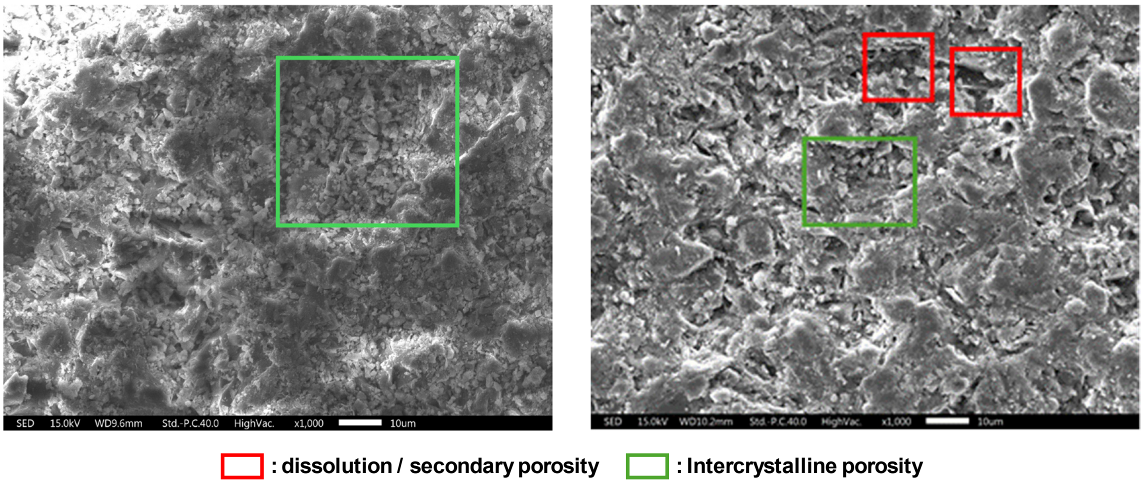

Figure 7
SEM results of ABF rock samples: (a) without CO_2 treatment; (b) 14 days of CO_2-brine soaking

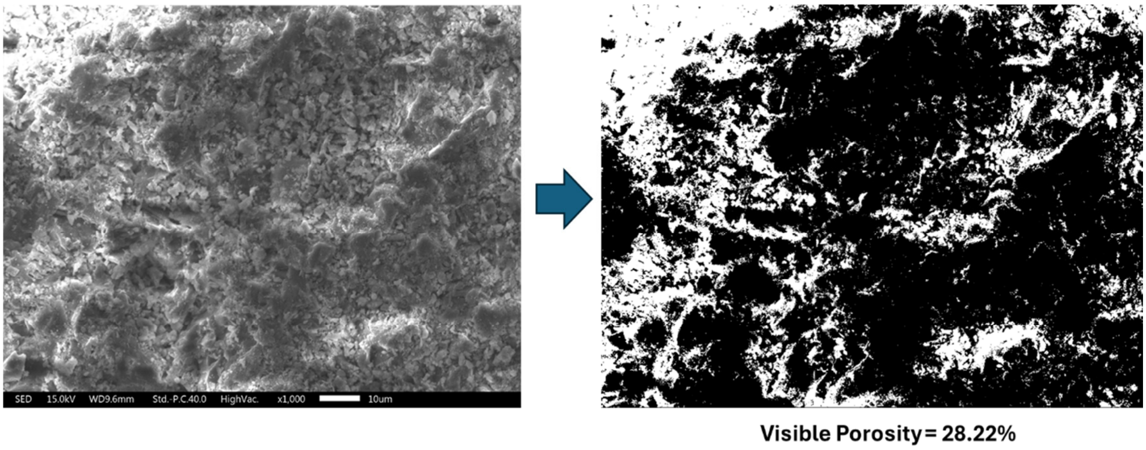

Figure 8
Visible porosity calculation for sample without CO_2 treatment, i.e. 28.22%

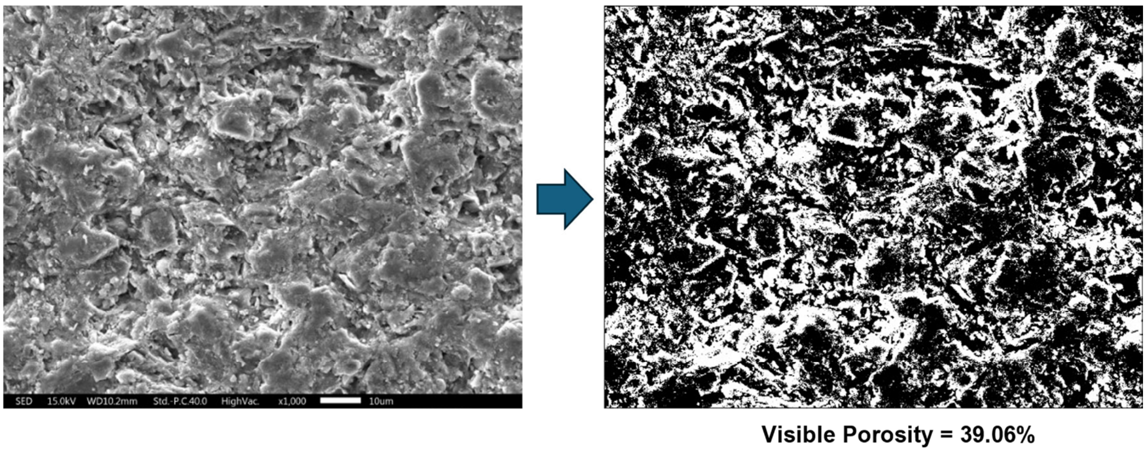

Figure 9
Visible porosity calculation for sample after soaked by CO_2-brine for 14 days i.e. 39.06% (~11% improvement compared with no CO_2-brine treatment)

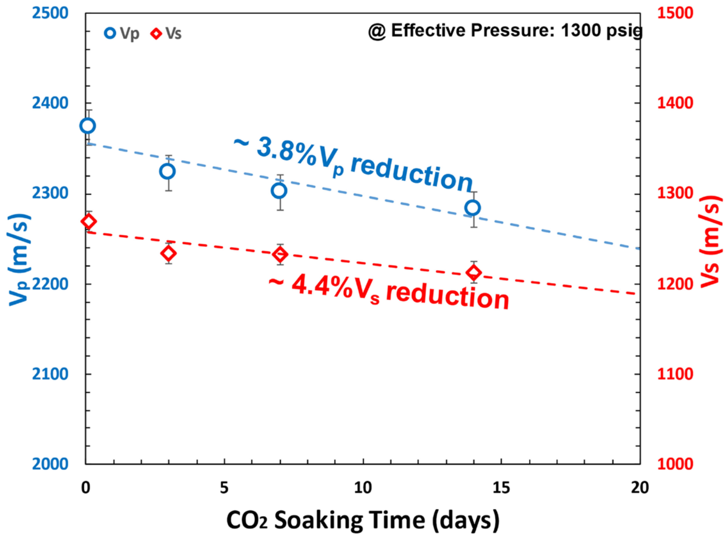

Figure 10
V_p and V_s measurements showed ~3.8% V_p and ~4.4% V_s reduction after soaked by CO2-brine for 14 days (measured at 1300 psig of effective pressure)

P & S Wave measurements

P & S Wave (V_p and V_s) measurements at 1300 psig of effective pressure are depicted in Figure 10. A reduction of ~3.8% of V_p and ~4.4% V_p was observed after being soaked by CO2-brine for 14 days. These results are aligned with previously reported experimental studies (Birch, 1943, 1960; Christensen, 1974; Christensen & Smewing, 1981; Mueller & Massonne, 2001; Kitamura et al., 2003; Nishimoto et al., 2005; Kern et al., 2008; Saito et al., 2015, 2016; Zhu et al., 2022; Creasy et al., 2024).

Geochemical Simulation

A simple line-drive model was used for geochemical simulation, as depicted in Figure 11. The observation cell was located at water producer well. The details of the simple line-drive model are shown in Table 3.

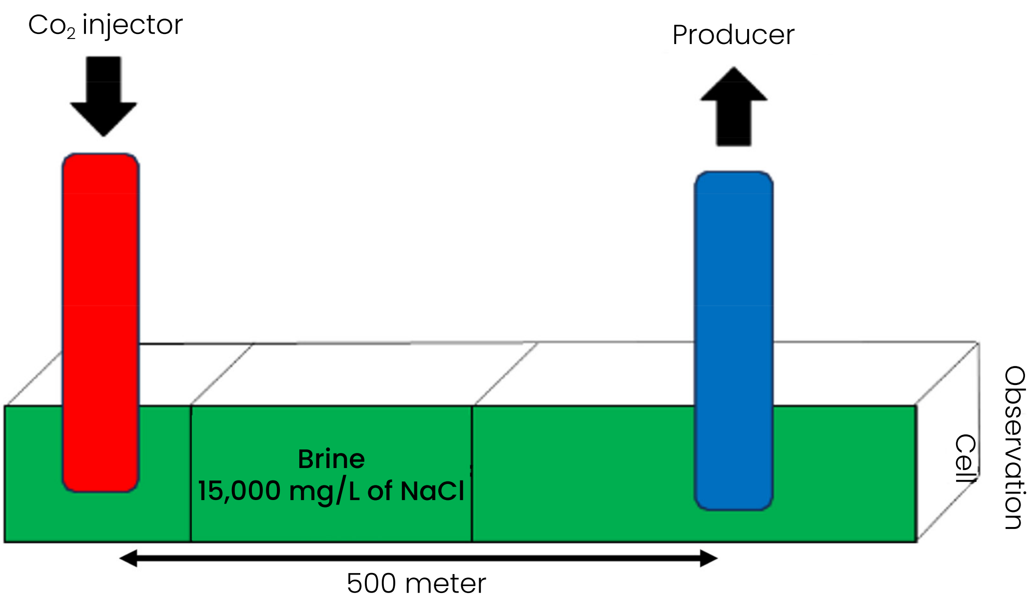

Figure 11
Simple line-drive model for geochemical simulation with 1 CO_2 injector well and 1 water producer well. The cell with water producer well was chosen as observation cell

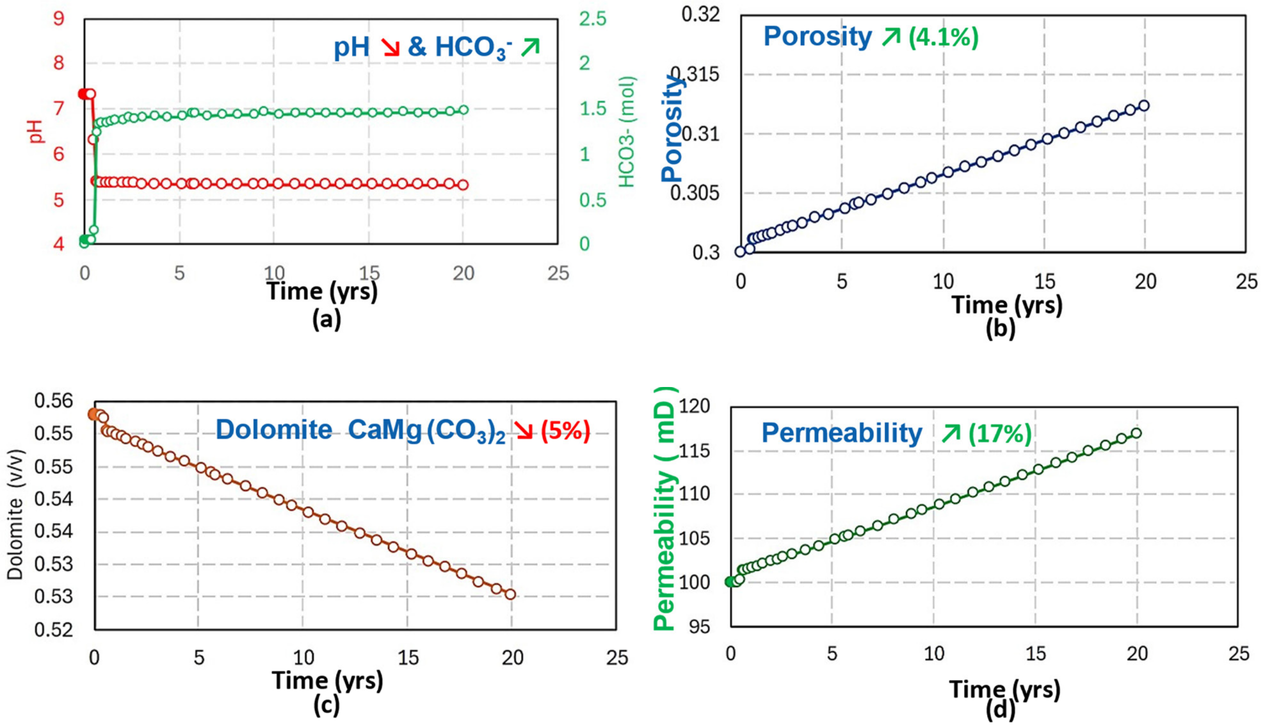

Figure 12
Results of geochemical simulation at observation cell: (a) pH and HCO3-; (b) porosity; (c) dolomite; (d) permeability

Table 3
Geochemical model properties

Initial reservoir pressure	psi	1300
Reservoir temperature	^{0}F	158
Porosity ϕ	-	0.3
Horizontal permeability (k_H)	mD	100
Vertical permeability (k_v)	mD	10
Dolomite	wt.%	79%
Quartz	wt.%	17%
Kaolinite	wt.%	4%
CO_2 injection rate	kg/s	100
Water production rate	kg/s	100

The results of the geochemical simulation of a simple line-drive model are depicted in Figure 12. pH reduction (from 7.30 to 5.50) as well as increasing of HCO3- are depicted in Figure 12(a). Figure 12(b) and Figure 12(d) show porosity (~4.1%) and permeability (~17%) improvements respectively, due to dolomite dissolution as shown in Figure 12(c).

Sand Onset Modelling

A simple homogeneous gas reservoir model was used as a case study of the producer pressure (reservoir pressure around the wellbore and bottom hole flowing pressure) profile. A commercial compositional reservoir simulator (Computer Modelling Group / CMG) was used to investigate CO2 injection performance (Peng-Robinson equation of state was used with 100% C1). Alteration of reservoir properties (such as porosity and permeability) due to geomechanic and geochemical effects was not modeled in this simulation.

A simple homogeneous reservoir model with a CO2 injector and a HC producer at grid model is depicted in Figure 13. The CO2 injector is perforated at the bottom of the grid model (k = 5) while the HC producer at the top of the grid model (k = 1).

Reservoir simulation results are shown in Figure 14 (producer well performance: CO2 mole rate, water rate, bottom hole pressure and near well reservoir pressure), Figure 15 (Pr vs Pwf on the producer for sand onset model) and Figure 16 (injector well performance: CO2 injection rate, bottom hole pressure and near well reservoir pressure), respectively. Water and CO2 breakthrough occurs at the producer well (as shown by Figure 14) which potentially forms of carbonic acid and leads to sand problem due to cementation dissolution.

Table 4
Synthetic reservoir model properties

Parameter	**Unit**	**Value**
Model size ($L_x \times L_y \times L_z$)	ft	$2500 \times 2500 \times 500$
Model dimension ($N_x \times N_y \times N_z$)	-	$5 \times 5 \times 5$
Grid top	ft	2900
Gas water contact (GWC)	ft	3050
Initial reservoir pressure	psi	1300
Reservoir temperature	^{0}F	158
Porosity ϕ	-	0.3
Horizontal permeability (k_H)	mD	100
Vertical permeability (k_v)	mD	10
Rock compressibility (c_r)	1/psi	3×10^{-6}
Water compressibility (c_w)	1/psi	2×10^{-6}
Initial gas saturation (S_{gi})	-	0.8
Irreducible water saturation (S_{wirr})	-	0.2
Residual gas saturation (S_{gr})	-	0.1
Max. gas relative permeability (k_{rg})	-	0.7
Max. water relative permeability (k_{rw})	-	0.7
Total pore volume	res. ft^3	9.413×10^8
Total hydrocarbon pore volume	res. ft^3	1.506×10^8
Original Gas in Place ($OGIP$)	std. ft^3	1.241×10^{10}
CO_2 injection rate	std.ft^3	3.00×10^6
Gas production rate	std.ft^3	3.00×10^6
Fracture pressure	psi	1652

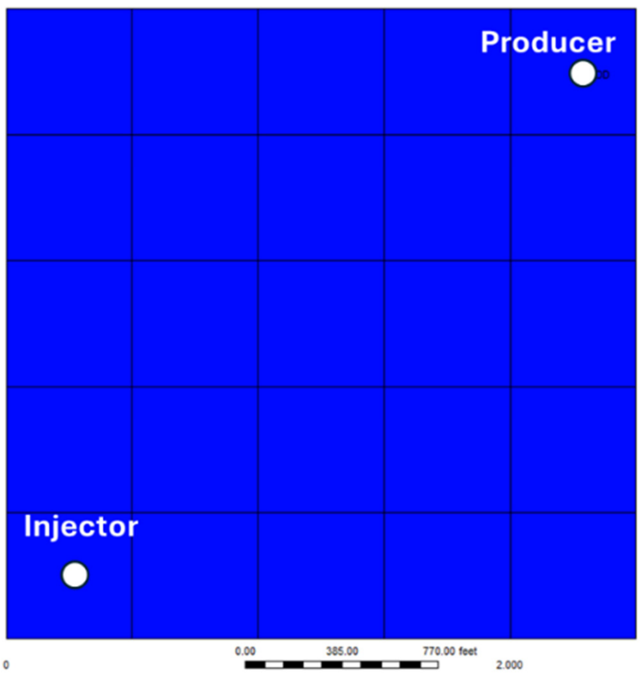

Figure 13
Simple synthetic homogeneous compositional model with 1 CO_2 injector and 1 gas producer

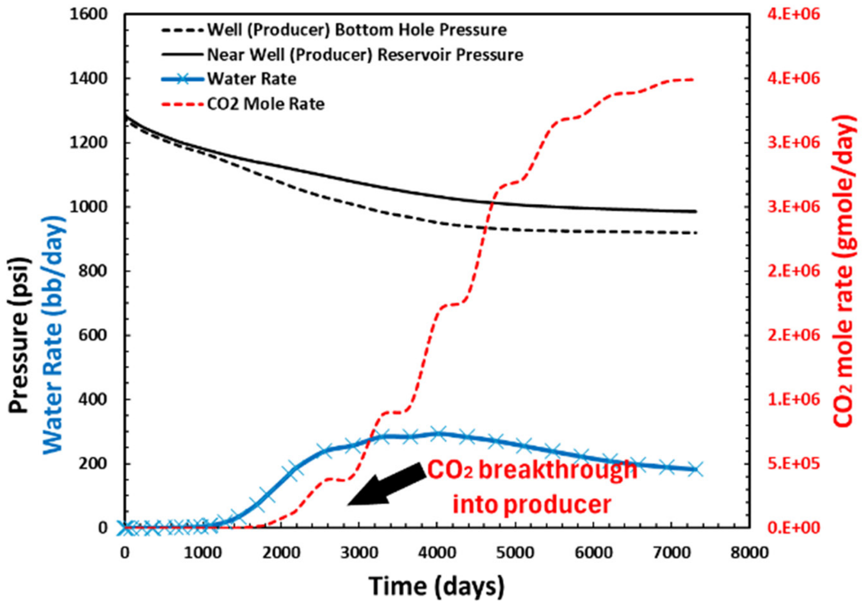

Figure 14
Compositional reservoir simulation results on producer well

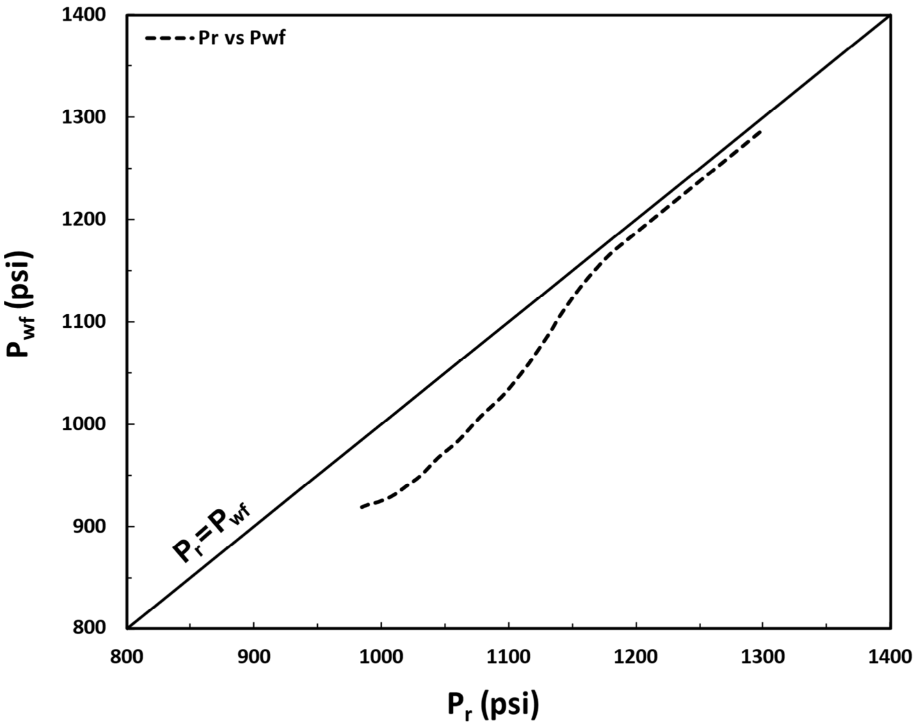

Figure 15
Pr vs Pwf on producer well

From elastic wave experimental results, sand onset criteria were constructed on the basis of the parameters shown in Table 5. This table clearly shows that rock strength was decreased after being soaked by CO2-brine (described in Young's modulus, UCS and TWC reduction after being soaked by CO2-brine). The sand onset model result for different cases are shown in Figure 17 and Figure 19. In Figure 17, for all production periods, the most likely sand problem would not have occurred in the producer well since Pr vs Pwf is still in green the area. On the other hand, Figure 19 shows that at late production time, sand problems would most likely occur in producer wells since Pwf is below CBHFP.

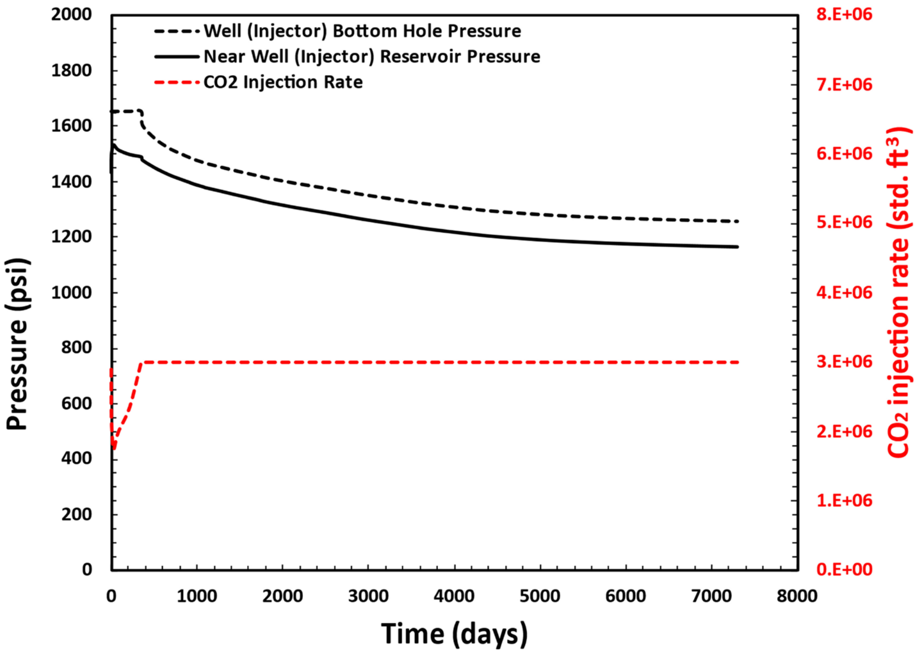

Figure 16
Simulation results on injector well

Table 5
Parameter of sand onset model

Parameter	Unit	Value
Initial (without CO_2 treatment)		
V_p	m/s	2374
V_s	m/s	1269
Poisson's ratio v	-	0.300
Young's modulus E	GPa	6.1
$UCS_{calculated}$	psi	1950
$TWC_{calculated}$	psi	5903
S_{hmin}@P_r = 1300 psig	psi	1814
S_{Hmax}@ P_r = 1300 psig	psi	2904
After being soaked by CO_2-brine for 14 days		
V_p	m/s	2271
V_s	m/s	1190
Poisson's ratio v	-	0.31
Young's modulus E	GPa	5.8
$UCS_{calculated}$	psi	1791
$TWC_{calculated}$	psi	5648
S_{hmin}@ P_r = 1300 psig	psi	1840
S_{Hmax}@ P_r = 1300 psig	psi	2987

The CBHFP comparison between with and without CO_2-brine-rock interactions is clearly shown in Figure 19. It is observed that CO_2-brine-rock affects rock strength reduction (from and reduction) and leads to more prone sand problems in producer wells. From the sand onset prediction model, it is shown that CO_2-brine-rock interactions would most likely increase sand problem risk in producer wells. Thus, this study demonstrates that considering CO_2-brine-rock interactions could help to design a better sand management strategy in producer wells. For further study, we suggest using experimental rock mechanics tests to obtain UCS or TWC if core samples are sufficient so that it will increase the accuracy of the sand onset prediction model.

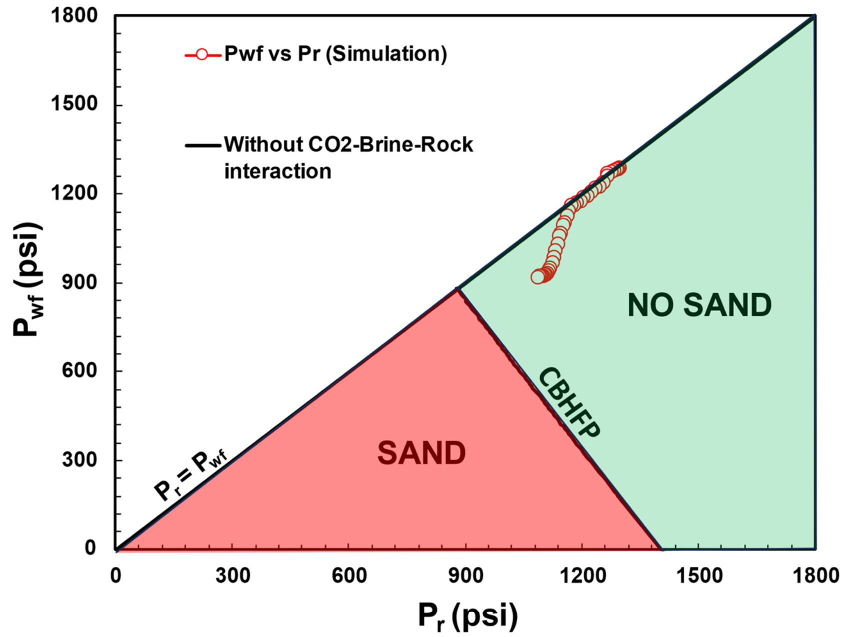

Figure 17
Sand onset model for initial case (without CO_2-brine-rock interaction)

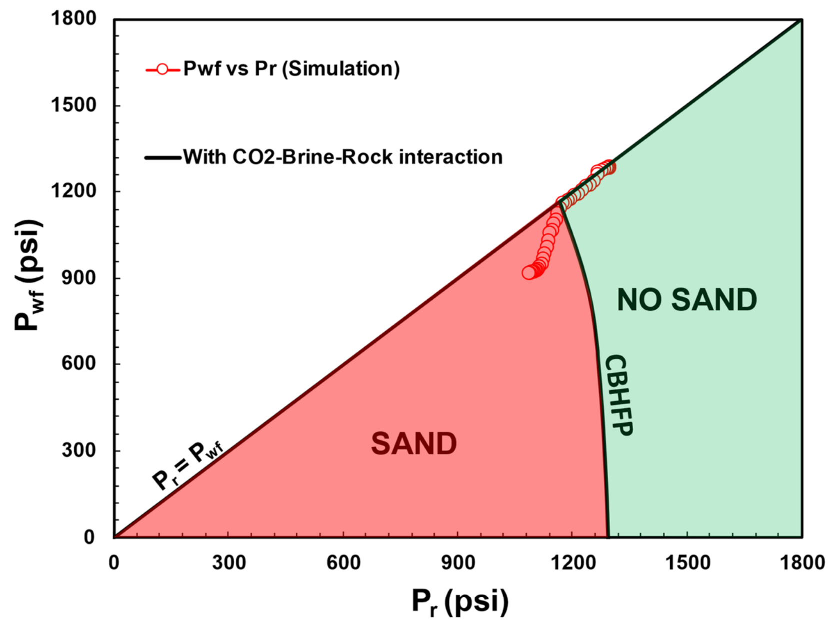

Figure 18
Sand onset model CO_2-brine soaking case (with CO_2-brine-rock interaction)

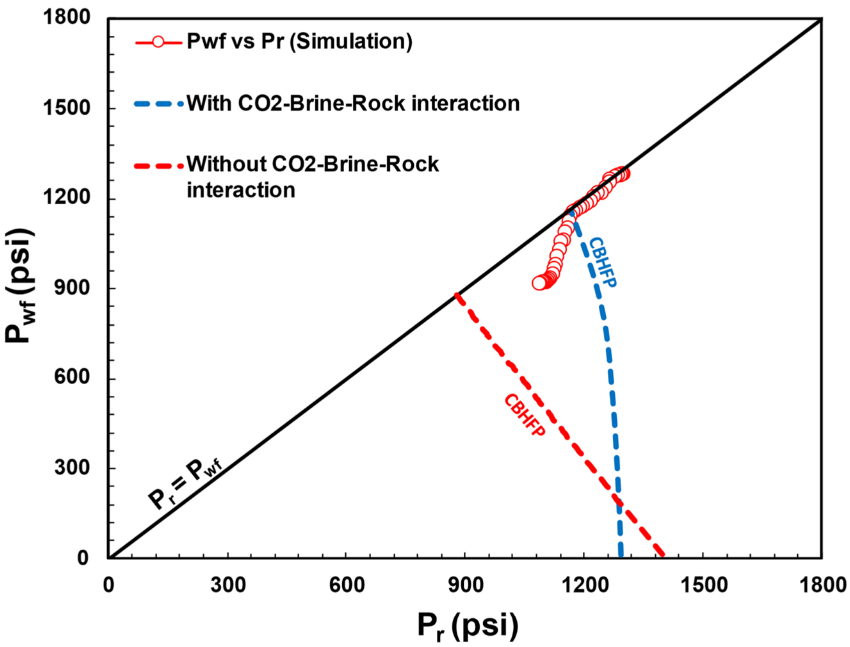

Figure 19
CBHFP model comparison between with and without CO_2-brine-rock interactions

CONCLUSION

Several experimental works have been conducted to investigate CO2-brine-rock interaction phenomena in dolomite-rich sandstone at Air Benakat Formation (ABF) by using CO2-brine-rock batch experiment setup. Indication of dolomite dissolution was observed by dry mass measurements, XRD, and SEM which leads to visible porosity improvement up to ~11% after being soaked by CO2-brine for 14 days.

Elastic wave velocity measurements resulting in and reduction (~ 3.8% of and ~ 4.4% of reduction at 1300 psi of effective pressure) after being soaked by CO2-brine for 14 days indirectly implies rock strength reduction due to CO2-brine-rock interactions.

The sand onset model was then constructed based on and experimental data by utilizing a simple reservoir simulation model as a case study of the producer well. From the sand onset prediction model, it is shown that CO2-brine-rock interactions would most likely increase sand problem risk in producer wells.

Thus, this study has demonstrated that considering CO2-brine-rock interactions could help to design a better sand management strategy in producer wells. For further study, we suggest using experimental rock mechanics tests to obtain UCS or TWC if core samples are sufficient, so that it will increase the accuracy of the sand onset prediction model.

ACKNOWLEDGEMENT

This research is supported and funded by LPPM Institut Teknologi Bandung (ITB) from “Riset Peningkatan Kapasitas Dosen Muda ITB 2022” funding scheme. Special appreciation is dedicated to Rock Fluid Imaging (RFI) laboratory teams (Susilowati, Irham Dzaky and teams) for helping conduct the experimental works.

GLOSSARY OF TERMS

Symbol	Definition	Unit
CBHFP	*Critical Bottom Hole Flowing Pressure*	*psi*
TWC	*Thick-Walled Cylinder*	*psi*
UCS	*Unconfined Compressive Strength*	*psi*
ϕ	*Porosity*	*[-]*

Symbol	Definition	Unit
S_{hmin}	*Horizontal minimum stress*	*psi*
S_{Hmax}	*Horizontal maximum stress*	*psi*
S_v	*Vertical stress*	*psi*
S_y	*Effective rock strength*	*psi*
E	*Young's modulus*	*GPa*
v	*Poisson's ratio*	*[-]*
ρ	*Rock density*	*kg/m^3*
V_p	*Compressional wave or P wave*	*m/s*
V_s	*Shear wave or S wave*	*m/s*
Δt	*Slowness*	$\mu s/ft$
P_r or P_p	*Reservoir or pore pressure*	*psi*
P_{wf} or BHP	*Well bottom hole pressure*	*psi*
fr_m	*m mineral volume fraction in rock*	*[-]*
fr_u	*non-reactive rock volume fraction*	*[-]*
k_{25}	*kinetic rate constant*	*mol/m^2/s*
E_a	*activation energi*	*KJ/mol*
α	*Biot's constant*	*[-]*
μ	*friction coefficient*	*[-]*
k_H	*Horizontal permeability*	*mD*
k_v	*Vertical permeability*	*mD*
c_r	*Rock compressibility*	*psi^{-1}*
c_w	*Water compressibility*	*psi^{-1}*
S_{gi}	*Initial gas saturation*	*[-]*
S_{wirr}	*Irreducible water saturation*	*[-]*
S_{gr}	*Residual gas saturation*	*[-]*
k_{rg}	*Max. gas relative permeability*	*[-]*
k_{rw}	*Max. water relative permeability*	*[-]*

REFERENCES

AL-Ameri, W.A. Abdulraheem, A. & Mahmoud, M., 2016, Long-Term Effects of CO2 Sequestration on Rock Mechanical Properties. Journal of Energy Resources Technology, 138(1), Article 1. https://doi.org/10.1115/1.4032011.

API RP40, 1998, API RP-40 Recommended Practice for Core Analysis.

Aziz, P.A., Marhaendrajana, T. & Siagian, U.W.R., 2023, Sanding phenomena vulnerability observations due to CO_2 injection at the Air Benakat reservoir in South Sumatera. Journal of Physics.

Aziz, P.A., Rachmat, M., Chandra, S., Daton, W.N. & Tony, B., 2023, Techno-Economic Solution For Extending Ccus Application In Natural Gas Fields: A Case Study Of B Gas Field In Indonesia. Scientific Contributions Oil and Gas, 46(1), 19–28. https://doi.org/10.29017/SCOG.46.1.1321.

Barber, A.J., Crow, M.J. & Milsom, J.S., 2005, Sumatra: Geology, Resources and Tectonic Evolution (Vol. 31).

Birch, F., 1943Elasticity of igneous rocks at high temperatures and pressures. Geological Society of America Bulletin, 54(2), 263–286. https://doi.org/10.1130/GSAB-54-263.

Birch, F., 1960, The velocity of compressional waves in rocks to 10 kilobars: 1. Journal of Geophysical Research, 65(4), 1083–1102. https://doi.org/10.1029/JZ065i004p01083.

Bishop, M.G., 2001, South Sumatra Basin Province, Indonesia: The Lahat/Talang Akar-Cenozoic Total Petroleum System (Open-File Report) [Open-File Report]. US Geological Survey (USGS).

Black, J.R., Carroll, S.A. & Haese, R.R., 2015, Rates of mineral dissolution under CO2 storage conditions. Chemical Geology, 399, 134–144. https://doi.org/10.1016/j.chemgeo.2014.09.020.

Bradford, I.D.R., Fuller, J., Thompson, P.J. & Walsgrove, T.R., 1998, Benefits of Assessing the Solids Production Risk in a North Sea Reservoir using Elastoplastic Modelling. All Days, SPE-47360-MS. https://doi.org/10.2118/47360-MS.

Breckels, I.M. & Van Eekelen, H.A.M., 1982, Relationship Between Horizontal Stress and Depth in Sedimentary Basins. Journal of Petroleum Technology, 34(09), 2191–2199. https://doi.org/10.2118/10336-PA.

Buhmann, D. & Dreybrodt, W., 1985, The kinetics of calcite dissolution and precipitation in geologically relevant situations of karst areas. Chemical Geology, 48(1–4), 189–211. https://doi.org/10.1016/0009-2541(85)90046-4.

Byerlee, J., 1978, Friction of rocks. Pure and Applied Geophysics, 116(4–5), 615–626. https://doi.org/10.1007/BF00876528.

Casey, W.H. & Sposito, G., 1992, On the temperature dependence of mineral dissolution rates. Geochimica et Cosmochimica Acta, 56(10), 3825–3830. https://doi.org/10.1016/0016-7037(92)90173-G.

Chang, C., Zoback, M.D. & Khaksar, A., 2006, Empirical relations between rock strength and physical properties in sedimentary rocks. Journal of Petroleum Science and Engineering, 51(3–4), 223–237. https://doi.org/10.1016/j.petrol.2006.01.003.

Christensen, N.I., 1974, Compressional wave velocities in possible mantle rocks to pressures of 30 kilobars. Journal of Geophysical Research, 79(2), 407–412. https://doi.org/10.1029/JB079i002p00407.

Christensen, N.I. & Smewing, J.D., 1981, Geology and seismic structure of the northern section of the Oman ophiolite. Journal of Geophysical Research: Solid Earth, 86(B4), 2545–2555. https://doi.org/10.1029/JB086iB04p02545.

Creasy, N., Huang, L., Gasperikova, E., Harbert, W., Bratton, T. & Zhou, Q. (2024). CO2 rock physics modeling for reliable monitoring of geologic carbon storage. Communications Earth & Environment, 5(1), 333. https://doi.org/10.1038/s43247-024-01493-6.

Crundwell, F.K., 2017, On the Mechanism of the Dissolution of Quartz and Silica in Aqueous Solutions. ACS Omega, 2(3), 1116–1127. https://doi.org/10.1021/acsomega.7b00019.

Dreybrodt, W. & Kaufmann, G., 2007, Physics and Chemistry of Dissolution on Subaerialy Exposed Soluble Rocks by Flowing Water Films. Acta Carsologica, 36(3). https://doi.org/10.3986/ac.v36i3.169.

Eaton, B.A., 1969, Fracture Gradient Prediction and Its Application in Oilfield Operations. Journal of Petroleum Technology, 21(10), 1353–1360. https://doi.org/10.2118/2163-PA.

Enick, R.M. & Klara, S.M., 1990, CO_2 Solubility In Water and Brine Under Reservoir Conditions. Chemical Engineering Communications, 90(1), 23–33. https://doi.org/10.1080/00986449008940574.

Fjaer, E. (Ed.), 2008, Petroleum related rock mechanics (2nd ed). Elsevier.

Golubev & Rabinovich, 1976, Resultaty primeneia appartury akusticeskogo karotasa dlja predeleina proconstych svoistv gornych porod na mestorosdeniaach tverdych isjopaemych. In Prikl. Geofiz. Moskva (Vol. 73, pp. 109–116).

Greenwood, N.N. & Earnshaw, A., 1997, Chemistry of the Elements. Elsevier. https://doi.org/10.1016/C2009-0-30414-6.

Gutierrez, M., Katsuki, D. & Almrabat, A., 2020, Seismic velocity change in sandstone during CO 2 injection. E3S Web of Conferences, 205, 02001. https://doi.org/10.1051/e3sconf/202020502001.

Holbrook, P.W., Maggiori, D.A. & Hensley, R., 1995, Real-Time Pore Pressure and Fracture-Pressure Determination in All Sedimentary Lithologies. SPE Formation Evaluation, 10(04), 215–222. https://doi.org/10.2118/26791-PA.

Horsrud, P., 2001, Estimating Mechanical Properties of Shale From Empirical Correlations. SPE Drilling & Completion, 16(02), 68–73. https://doi.org/10.2118/56017-PA.

Hubbert, M.K. & Willis, D.G., 1957, Mechanics Of Hydraulic Fracturing. Transactions of the AIME, 210(01), 153–168. https://doi.org/10.2118/686-G.

IPCC., 2005, Carbon Dioxide Capture and Storage. Cambridge University Press. https://www.ipcc.ch/report/carbon-dioxide-capture-and-storage/

Jaeger & Cook, N.G.W., 1979, Fundamentals of Rock Mechanics. Geological Magazine, 117(4), 401–401. https://doi.org/10.1017/S001675680003274X.

Kern, H., Ivankina, T.I., Nikitin, A.N., Lokajíček, T. & Pros, Z., 2008, The effect of oriented microcracks and crystallographic and shape preferred orientation on bulk elastic anisotropy of a foliated biotite gneiss from Outokumpu. Tectonophysics, 457(3–4), 143–149. https://doi.org/10.1016/j.tecto.2008.06.015.

Khaksar, A., Asadi, S., Younessi, A., Gui, F. & Zheng, Y. (2018). Thick Wall Cylinder Strength And Critical Strain Limit from Core Tests And Well Logs, Implications for Sand Control Decisions.

Kitamura, K., Ishikawa, M. & Arima, M., 2003, Petrological model of the northern Izu–Bonin–Mariana arc crust: Constraints from high-pressure measurements of elastic wave velocities of the Tanzawa plutonic rocks, central Japan. Tectonophysics, 371(1–4), 213–221. https://doi.org/10.1016/S0040-1951(03)00229-4.

Lal, M., 1999, Shale Stability: Drilling Fluid Interaction and Shale Strength. SPE Asia Pacific Oil and Gas Conference and Exhibition, SPE-54356-MS. https://doi.org/10.2118/54356-MS.

Lamy-Chappuis, B., Angus, D., Fisher, Q.J. & Yardley, B.W.D., 2016). The effect of CO 2 -enriched brine injection on the mechanical properties of calcite-bearing sandstone. International Journal of Greenhouse Gas Control, 52, 84–95. https://doi.org/10.1016/j.ijggc.2016.06.018.

Lerman, A. & Mackenzie, F.T., 2018, Carbonate minerals and the CO2-carbonic acid system. In Encyclopedia of Earth Sciences Series. Springer.

Luquot, L., Rodriguez, O. & Gouze, P., 2014, Experimental Characterization of Porosity Structure and Transport Property Changes in Limestone Undergoing Different Dissolution Regimes. Transport in Porous Media, 101(3), 507–532. https://doi.org/10.1007/s11242-013-0257-4.

Matter, J.M., Takahashi, T. & Goldberg, D., 2007, Experimental evaluation of in situ CO_2 -water-rock reactions during CO_2 injection in basaltic rocks: Implications for geological CO_2 sequestration. Geochemistry, Geophysics, Geosystems, 8(2), 2006GC001427. https://doi.org/10.1029/2006GC001427.

Matthews, W.R. & Kelly, J., 1967, How to Predict Formation Pressure and Fracture Gradient. Oil and Gas Journal, 65, 92–1066.

McPhee, C., Reed, J. & Zubizarreta, I., 2015, Core Sample Preparation. In Developments in Petroleum Science (Vol. 64, pp. 135–179). Elsevier. https://doi.org/10.1016/B978-0-444-63533-4.00004-4.

Militzer & Stoll., 1973, Einige Beitrageder geophysics zur primadatenerfassung im Bergbau (Vol. 3). Neue Bergbautechnik.

Mitchell, M.J., Jensen, O.E., Cliffe, K.A. & Maroto-Valer, M.M., 2010, A model of carbon dioxide dissolution and mineral carbonation kinetics. Proceedings of the Royal Society A: Mathematical, Physical and Engineering Sciences, 466(2117), 1265–1290. https://doi.org/10.1098/rspa.2009.0349.

Moos, D., Zoback, M.D. & Bailey, L., 1999, Feasibility Study of the Stability of Openhole Multilaterals, Cook Inlet, Alaska. All Days, SPE-52186-MS. https://doi.org/10.2118/52186-MS.

Mueller, H.J. & Massonne, H.-J., 2001, Experimental high pressure investigation of partial melting in natural rocks and their influence on Vp and Vs. Physics and Chemistry of the Earth, Part A: Solid Earth and Geodesy, 26(4–5), 325–332. https://doi.org/10.1016/S1464-1895(01)00062-X.

Nakajima, T. & Xue, Z., 2021, Hysteretic Behavior in the Relationship Between Vp and CO2 Saturation Obtained From the Time-lapse Logging at the Nagaoka Site. SSRN Electronic Journal. https://doi.org/10.2139/ssrn.3818070.

Nishimoto, S., Ishikawa, M., Arima, M. & Yoshida, T., 2005, Laboratory measurement of P-wave velocity in crustal and upper mantle xenoliths from Ichino-megata, NE Japan: Ultrabasic hydrous lower crust beneath the NE Honshu arc. Tectonophysics, 396(3–4), 245–259. https://doi.org/10.1016/j.tecto.2004.12.010.

Nugraha, F.Y., Al Hakim, M.F., Tony, B., Nandiwardhana, D. & Chandra, S. (2024). Development of CO_2 Hub-Clustering Management in The South Sumatra Basin. Scientific Contributions Oil and Gas, 47(1), 31–40. https://doi.org/10.29017/SCOG.47.1.1607.

Nurhandoko, B.E., 2022, Perangkat Pengukuran Gelombang P Dan Gelombang S Yang Murni, Akurat Dan Rendah Derau (Patent IDP000046083).

Nurhandoko, B.E.B. & Listyobudi, M., 2018, Thick Walled Core Testing for Sanding Analysis of Chalky Carbonate Reservoir in Production Borehole. Annual Scientific Meeting Himpunan Ahli Geofisika Indonesia. Annual Scientific Meeting Himpunan Ahli Geofisika Indonesia, Semarang, Indonesia.

Nurhandoko, B.E.B., Rizka Asmara Hadi, M., Triyoso, K., Martha, R.K., Widowati, S., Sukrisna, B., Syamsuddin & Romli, N.I., 2021, Sanding Wells on The Island of Lombok due to Earthquake Vibrations. IOP Conference Series: Earth and Environmental Science, 873(1), 012091. https://doi.org/10.1088/1755-1315/873/1/012091.

Palmer, I., Vaziri, H., Willson, S., Moschovidis, Z., Cameron, J. & Ispas, I., 2003, Predicting and Managing Sand Production: A New Strategy. All Days, SPE-84499-MS. https://doi.org/10.2118/84499-MS.

Rahman, K., Khaksar, A. & Kayes, T., 2010, An Integrated Geomechanical and Passive Sand-Control Approach to Minimizing Sanding Risk From Openhole and Cased-and-Perforated Wells. SPE Drilling & Completion, 25(02), 155–167. https://doi.org/10.2118/116633-PA.

Rathnaweera, T.D., Ranjith, P.G., Perera, M.S.A., Ranathunga, A.S., Wanniarachchi, W.A.M., Yang, S. Q., Lashin, A. & Al Arifi, N., 2017, An experimental investigation of coupled chemico-mineralogical and mechanical changes in varyingly-cemented sandstones upon CO2 injection in deep saline aquifer environments. Energy, 133, 404–414. https://doi.org/10.1016/j.energy.2017.05.154.

Saito, S., Ishikawa, M., Arima, M. & Tatsumi, Y., 2015, Laboratory measurements of 'porosity-free' intrinsic V p and V s in an olivine gabbro of the O man ophiolite: Implication for interpretation of the seismic structure of lower oceanic crust. Island Arc, 24(2), 131–144. https://doi.org/10.1111/iar.12092.

Saito, S., Ishikawa, M., Arima, M. & Tatsumi, Y., 2016, Laboratory measurements of Vp and Vs in a porosity-developed crustal rock: Experimental investigation into the effects of porosity at deep crustal pressures. Tectonophysics, 677–678, 218–226. https://doi.org/10.1016/j.tecto.2016.03.044.

Slobod, R.L., Chambers, A. & Prehn, W.L., 1951, Use of Centrifuge for Determining Connate Water, Residual Oil, and Capillary Pressure Curves of Small Core Samples. Journal of Petroleum Technology, 3(04), 127–134. https://doi.org/10.2118/951127-G.

Spycher, N., Pruess, K., & Ennis-King, J., 2003, CO_2-H_2O mixtures in the geological sequestration of CO_2. I. Assessment and calculation of mutual solubilities from 12 to 100°C and up to 600 bar. Geochimica et Cosmochimica Acta, 67(16), Article 16. https://doi.org/10.1016/S0016-7037(03)00273-4.

Sugihardjo, S., 2022, CCUS-Aksi Mitigasi Gas Rumah Kaca dan Peningkatan Pengurasan Minyak CO2-EOR. Lembaran publikasi minyak dan gas bumi, 56(1), 21–35. https://doi.org/10.29017/LPMGB.56.1.916.

Vaziri, H., Xiao, Y. & Palmer, I., 2002, Assessment Of Several Sand Prediction Models With Particular Reference To HPHT Wells. All Days, SPE-78235-MS. https://doi.org/10.2118/78235-MS.

Willson, S.M., Moschovidis, Z.A., Cameron, J.

R. & Palmer, I. D. (2002). New Model for Predicting the Rate of Sand Production. SPE/ISRM Rock Mechanics Conference. https://doi.org/10.2118/78168-MS.

Xu, T., Sonnenthal, E., Spycher, N. & Pruess, K., 2006, Toughreact—A simulation program for non-isothermal multiphase reactive geochemical transport in variably saturated geologic media: Applications to geothermal injectivity and CO2 geological sequestration. Computers & Geosciences, 32(2), 145–165. https://doi.org/10.1016/j.cageo.2005.06.014.

Xu, T., Sonnenthal, E., Spycher, N. & Zheng, L., 2014, Toughreact_V3-OMP_SampleProblems.

Yu, Z., Yang, S., Liu, K., Zhuo, Q. & Yang, L., 2019, An Experimental and Numerical Study of CO_2–Brine-Synthetic Sandstone Interactions under High-Pressure (P)–Temperature (T) Reservoir Conditions. Applied Sciences, 9(16), 3354. https://doi.org/10.3390/app9163354.

Zhang, G., Spycher, N., Xu, T., Sonnenthal, E. & Steefel, C. (2006). Reactive Geochemical Transport Modeling of Concentrated AqueousSolutions: Supplement to Toughreact User's Guide for the PitzerIon-Interaction Model (LBNL--62718, 919388; p. LBNL--62718, 919388). https://doi.org/10.2172/919388.

Zhu, S., Kang, J., Wang, Y. & Zhou, F., 2022), Effect of CO_2 on coal P-wave velocity under triaxial stress. International Journal of Mining Science and Technology, 32(1), 17–26. https://doi.org/10.1016/j.ijmst.2021.09.006.

Zoback, 2007, Reservoir geomechanics. Cambridge University Press.

Zoback, M.D. & Healy, J.H., 1984, Friction, faulting and in situ stress. Annales Geophysicae (1983), 2, 689–698.